

# A non-perturbative analysis of symmetry breaking in two-dimensional $\phi^4$ theory using periodic field methods

Pablo J. Marrero\*, Erick A. Roura† and Dean Lee‡  
 Department of Physics and Astronomy  
 University of Massachusetts, Amherst, MA 01003

October 9, 2018

## Abstract

We describe the generalization of spherical field theory to other modal expansion methods. The main approach remains the same, to reduce a  $d$ -dimensional field theory into a set of coupled one-dimensional systems. The method we discuss here uses an expansion with respect to periodic-box modes. We apply the method to  $\phi^4$  theory in two dimensions and compute the critical coupling and critical exponents. We compare with lattice results and predictions via universality and the two-dimensional Ising model. [PACS numbers: 05.10-a, 05.50+q, 11.10.-z, 11.30.Qc, 12.38Lg]

## 1 Introduction

Recently spherical field theory has been introduced as a non-perturbative method for studying quantum field theory [1]. The starting point of this approach is to decompose field configurations in a  $d$ -dimensional Euclidean functional integral as linear combinations of spherical partial waves. Regarding each partial wave as a distinct field in a new one-dimensional system, the functional integral is rewritten as a time-evolution equation, with radial distance serving as the parameter of time. The core idea of spherical field theory is to reduce quantum field theory to a set of coupled quantum-mechanical systems. The technique used is partial wave decomposition, but this can easily be generalized to other modal expansions. Instead of concentric spheres and partial waves, we might instead consider a generic smooth one-parameter family of  $(d - 1)$ -dimensional

---

\*email: marrero@het.phast.umass.edu

†email: roura@het.phast.umass.edu

‡email: dlee@het.phast.umass.edu

manifolds (disjoint and compact) and basis functions defined over each manifold. There are clearly many possibilities and we can optimize our expansion scheme to suit the specific problem at hand.

One important and convenient feature of spherical field theory is that it eliminates the need to compactify space — the spherical quantization surface is already compact. This is useful for studying phenomena which might be influenced by our choice of boundary conditions, such as topological excitations. Another interesting example arises in the process of quantization on noncommutative geometries. Spherical field methods have recently been adapted to study quantum field theory on the noncommutative plane [2]. In many instances, however, maintaining exact translational invariance is of greater value than non-compactness or exact rotational invariance. In that case one could consider a system whose spatial dimensions have been compactified to form a periodic box. The next step would be to expand field configurations using free modes of the box and evolve in time. We will refer to this arrangement as periodic-mode field theory or, more simply, periodic field theory.<sup>1</sup>

In periodic field theory the Hamiltonian is time independent and linear momentum is exactly conserved. In this work we describe the basic features of periodic field theory and use it to analyze spontaneous symmetry breaking in Euclidean two-dimensional  $\phi^4$  theory. We use the method of diffusion Monte Carlo to simulate the dynamics of the theory. The techniques discussed here have several advantages over conventional Euclidean lattice Monte Carlo methods. One is that periodic boundary conditions are not imposed on the time variable, making it easier to determine the particle mass from an exponential decay fit. Another is that the zero-momentum mode is regarded as a single degree of freedom (rather than a collective mode on the lattice), which provides a simpler description of vacuum expectation values and symmetry breaking. Other advantages arise in systems not considered here, such as the absence of fermion doubling and extensions to Minkowski space using non-stochastic computational methods.

The organization of this paper is as follows. We begin with a derivation of periodic field theory. We then analyze two-dimensional  $\phi^4$  theory and its corresponding periodic-field Hamiltonian using diffusion Monte Carlo methods. We compute the critical coupling at which  $\phi \rightarrow -\phi$  reflection symmetry is broken, and determine the critical exponents  $\nu$  and  $\beta$ .<sup>2</sup> We find that our value of the critical coupling is in agreement with recent lattice results [7], and our values for the critical exponents are consistent with predictions via universality and the two-dimensional Ising model.

---

<sup>1</sup>Periodic field theory could be viewed as a hybrid of the Hamiltonian and momentum-space lattice formalisms. This combination, however, has not been discussed in the literature.

<sup>2</sup>We are using standard notation.  $\nu$  is associated with the inverse correlation length, and  $\beta$  corresponds with the behavior of the vacuum expectation value of  $\phi$ .

## 2 Periodic fields

We start with free scalar field theory in two dimensions subject to periodic boundary conditions

$$\phi(t, x - L) = \phi(t, x + L). \quad (1)$$

In our discussion  $t$  is Euclidean time, analytically continued from imaginary Minkowskian time. Let  $\mathcal{J}$  be an external source satisfying the same boundary conditions and which vanishes as  $|t| \rightarrow \infty$ . The Euclidean generating functional in the presence of  $\mathcal{J}$  is given by

$$Z[\mathcal{J}] \propto \int \mathcal{D}\phi \exp \left\{ -\int_{-\infty}^{\infty} dt \int_{-L}^L dx \left[ \frac{1}{2} \left( \left( \frac{\partial \phi}{\partial t} \right)^2 + \left( \frac{\partial \phi}{\partial x} \right)^2 \right) + \frac{\mu^2}{2} \phi^2 - \mathcal{J}\phi \right] \right\}. \quad (2)$$

We now expand in terms of periodic-box modes,

$$\begin{aligned} \phi(t, x) &= \sqrt{\frac{1}{2L}} \sum_{n=0, \pm 1, \dots} \phi_n(t) e^{in\pi x/L}, \\ \mathcal{J}(t, x) &= \sqrt{\frac{1}{2L}} \sum_{n=0, \pm 1, \dots} \mathcal{J}_n(t) e^{in\pi x/L}. \end{aligned} \quad (3)$$

These are also eigenmodes of momentum and each  $\phi_n$  or  $\mathcal{J}_n$  carries momentum  $\frac{n\pi}{L}$ . In terms of these modes, we have

$$Z[\mathcal{J}] \propto \int \prod_n \mathcal{D}\phi_n \exp \left\{ -\int_{-\infty}^{\infty} dt \sum_n \left[ \frac{1}{2} \frac{d\phi_{-n}}{dt} \frac{d\phi_n}{dt} + \frac{1}{2} \left( \frac{n^2 \pi^2}{L^2} + \mu^2 \right) \phi_{-n} \phi_n - \mathcal{J}_{-n} \phi_n \right] \right\}. \quad (4)$$

For notational purposes we will define

$$\omega_n = \sqrt{\frac{n^2 \pi^2}{L^2} + \mu^2}. \quad (5)$$

Using the Feynman-Kac formula, we find

$$Z[\mathcal{J}] \propto \langle 0 | T \exp \left\{ -\int_{-\infty}^{\infty} dt H_{\mathcal{J}} \right\} | 0 \rangle, \quad (6)$$

where

$$H_{\mathcal{J}} = \sum_n \left[ -\frac{1}{2} \frac{\partial}{\partial q_{-n}} \frac{\partial}{\partial q_n} + \frac{1}{2} \omega_n^2 q_{-n} q_n - \mathcal{J}_{-n} q_n \right], \quad (7)$$

and  $|0\rangle$  is the ground state of  $H_0$ . Since  $H_0$  is the usual equal time Hamiltonian,  $|0\rangle$  is the vacuum.  $H_0$  consists of a set of decoupled harmonic oscillators, and it is straightforward to calculate the two-point correlation functions,

$$\langle 0 | \phi_{-n}(t_2) \phi_n(t_1) | 0 \rangle = \frac{\delta}{\delta \mathcal{J}_n(t_2)} \frac{\delta}{\delta \mathcal{J}_{-n}(t_1)} Z[\mathcal{J}] \Big|_{\mathcal{J}=0} = \frac{1}{2\omega_n} \exp[-\omega_n |t_2 - t_1|]. \quad (8)$$

We now include a  $\phi^4$  interaction term as well as a counterterm Hamiltonian, which we denote as  $H_{c.t.}$ . The new Hamiltonian is

$$H_{\mathcal{J}} = \sum_n \left[ -\frac{1}{2} \frac{\partial}{\partial q_{-n}} \frac{\partial}{\partial q_n} + \frac{1}{2} \omega_n^2 q_{-n} q_n - \mathcal{J}_{-n} q_n \right] + \frac{\lambda}{4!2L} \sum_{n_1+n_2+n_3+n_4=0} q_{n_1} q_{n_2} q_{n_3} q_{n_4} + H_{c.t.}. \quad (9)$$

We will regulate the sums over momentum modes by choosing some large positive number  $N_{\max}$  and throwing out all high-momentum modes  $q_n$  such that  $|n| > N_{\max}$ . This corresponds to a momentum cutoff

$$\Lambda^2 = \left( \frac{N_{\max} \pi}{L} \right)^2. \quad (10)$$

In two-dimensional  $\phi^4$  theory, renormalization can be implemented by normal ordering the  $\phi^4$  interaction term. This corresponds to cancelling diagrams of the type shown in Figure 1. Using (8), we find

$$H_{c.t.} = \frac{6\lambda b}{4!2L} \sum_{n=-N_{\max}, N_{\max}} q_{-n} q_n, \quad (11)$$

where

$$b = \sum_{n=-N_{\max}, N_{\max}} \frac{1}{2\omega_n}. \quad (12)$$

For the remainder of our discussion we will use the Hamiltonian

$$H = H_0 = \sum_n \left[ -\frac{1}{2} \frac{\partial}{\partial q_{-n}} \frac{\partial}{\partial q_n} + \frac{1}{2} (\omega_n^2 - \frac{\lambda b}{4L}) q_{-n} q_n \right] + \frac{\lambda}{4!2L} \sum_{n_1+n_2+n_3+n_4=0} q_{n_1} q_{n_2} q_{n_3} q_{n_4}. \quad (13)$$

### 3 The $\phi_2^4$ phase transition

The existence of a second-order phase transition in two-dimensional  $\phi^4$  theory has been derived in the literature [3][4]. The phase transition is due to  $\phi$  developing a non-zero expectation value and the resultant spontaneous breaking of  $\phi \rightarrow -\phi$  reflection symmetry. It is generally believed that this theory belongs to the same universality class as the two-dimensional Ising model and therefore shares the same critical exponents. In this section we apply periodic field methods to  $\phi^4$  theory in order to determine the critical coupling and critical exponents  $\nu$  and  $\beta$ . We have chosen  $\nu$  and  $\beta$  since these are, in our opinion, the easiest to determine from direct computations. All other exponents can be derived from these using well-known scaling laws. From the Ising model predictions we expect

$$\nu = 1, \quad \beta = \frac{1}{8}. \quad (14)$$

$\nu$  is the exponent associated with the inverse correlation length or, equivalently, the mass of the one-particle state. We will determine the behavior of the mass as we approach the critical point from the symmetric phase of the theory.

Let  $|a\rangle$  be any state even under reflection symmetry. We consider the matrix element

$$f(t) = \langle a | q_0 \exp(-tH) q_0 | a \rangle. \quad (15)$$

Inserting energy eigenstates  $|i\rangle$  satisfying  $H|i\rangle = E_i|i\rangle$ , we have

$$f(t) = \sum_i \exp(-tE_i) |\langle i | q_0 | a \rangle|^2. \quad (16)$$

Since  $|a\rangle$  and  $|0\rangle$  are even under reflection symmetry and  $q_0$  is odd, the vacuum contribution to the sum in (16) vanishes. In the limit  $t \rightarrow \infty$ , (16) is dominated by the contribution of the next lowest energy state, the one-particle state at rest.<sup>3</sup> In this limit we have

$$f(t) \sim e^{-mt}, \quad (17)$$

where  $m$  is the mass. We can compute  $f(t)$  numerically using the method of diffusion Monte Carlo (DMC). The idea of DMC is to model the dynamics of the imaginary-time Schrödinger equation using the diffusion and decay/production of simulated particles. The kinetic energy term in the Hamiltonian determines the diffusion rate of the particles (usually called replicas) and the potential energy term determines the local decay/production rate. A self-contained introduction to DMC can be found in [5].

$\nu$  is defined by the behavior of  $m$  near the critical coupling  $\lambda_c$ ,

$$m \sim (\lambda_c - \lambda)^\nu. \quad (18)$$

Once we determine  $f(t)$  using DMC simulations we can extract  $m$  and  $\nu$  using curve-fitting techniques. We have calculated  $m$  as a function of  $\lambda$  for several different values of  $L$  and  $N_{\max}$ . Results from these calculations are presented in the next section.

$\beta$  is the critical exponent describing the behavior of the vacuum expectation value. In the symmetric phase the vacuum state is unique and invariant under the reflection transformation  $\phi \rightarrow -\phi$  (or equivalently  $q_n \rightarrow -q_n$ , for each  $n$ ). In the broken-symmetry phase the vacuum is degenerate as  $L \rightarrow \infty$ , and  $q_0$ , the zero-momentum mode, develops a vacuum expectation value. In the  $L \rightarrow \infty$  limit tunnelling between vacuum states is forbidden. One ground state,  $|0^+\rangle$ , is non-zero only for values  $q_0 > 0$  and the other,  $|0^-\rangle$ , is non-zero only for  $q_0 < 0$ . We will choose  $|0^+\rangle$  and  $|0^-\rangle$  to be unit normalized.

Let us now define the symmetric and antisymmetric combinations,

$$\begin{aligned} |0^s\rangle &= \frac{1}{\sqrt{2}} (|0^+\rangle + |0^-\rangle) \\ |0^a\rangle &= \frac{1}{\sqrt{2}} (|0^+\rangle - |0^-\rangle). \end{aligned} \quad (19)$$

---

<sup>3</sup>We are assuming that this contribution does not also vanish. This is generally true, and we can always vary  $|a\rangle$  to make it so.

We will select the relative phases of  $|0^-\rangle$  and  $|0^+\rangle$  so that they transform from one to the other under reflection symmetry.  $|0^s\rangle$  and  $|0^a\rangle$  are then symmetric and antisymmetric (respectively) under reflection symmetry.

To avoid notational confusion in the following, we will write  $\hat{q}_n$  to denote the quantum-mechanical position operator and  $q_n$  for the corresponding ordinary variable. Let  $\left\{ \hat{\mathcal{P}}_z \right\}_{z \in (-\infty, \infty)}$  be the spectral family associated with the operator  $\frac{\hat{q}_0}{\sqrt{2L}}$ .<sup>4</sup> This implies that  $\int_a^b d\hat{\mathcal{P}}_z$  is a projection operator whose action on a general wavefunction  $\Psi$  is

$$\left( \int_a^b d\hat{\mathcal{P}}_z \right) \Psi(q_0, q_1, \dots) = \theta\left(-\frac{q_0}{\sqrt{2L}} - a\right) \theta\left(b - \frac{q_0}{\sqrt{2L}}\right) \Psi(q_0, q_1, \dots). \quad (20)$$

From the support properties of  $|0^+\rangle$  and  $|0^-\rangle$ , we deduce

$$\begin{aligned} |0^+\rangle &= \sqrt{2} \int_0^\infty d\hat{\mathcal{P}}_z |0^s\rangle = \sqrt{2} \int_0^\infty d\hat{\mathcal{P}}_z |0^a\rangle \\ |0^-\rangle &= \sqrt{2} \int_{-\infty}^0 d\hat{\mathcal{P}}_z |0^s\rangle = -\sqrt{2} \int_{-\infty}^0 d\hat{\mathcal{P}}_z |0^a\rangle. \end{aligned} \quad (21)$$

Using our new spectral language, we can write

$$\frac{\hat{q}_0}{\sqrt{2L}} = \int_{-\infty}^\infty z d\hat{\mathcal{P}}_z. \quad (22)$$

We now consider the vacuum expectation value  $\langle 0^+ | \phi | 0^+ \rangle$ .<sup>5</sup> Making use of translational invariance, we have

$$\langle 0^+ | \phi | 0^+ \rangle = \frac{1}{2L} \int_{-L}^L dx \langle 0^+ | \phi(t, x) | 0^+ \rangle = \langle 0^+ | \frac{\hat{q}_0}{\sqrt{2L}} | 0^+ \rangle. \quad (23)$$

From (21) and (22), we conclude that

$$\langle 0^+ | \phi | 0^+ \rangle = 2 \langle 0^s | \int_0^\infty z d\hat{\mathcal{P}}_z | 0^s \rangle = 2 \int_0^\infty dz z g(z), \quad (24)$$

where

$$g(z) = \langle 0^s | \frac{d\hat{\mathcal{P}}_z}{dz} | 0^s \rangle. \quad (25)$$

$g(z)$  satisfies the normalization condition

$$\int_{-\infty}^\infty dz g(z) = 2 \int_0^\infty dz g(z) = 1. \quad (26)$$

In our calculations we will be working with large but finite  $L$ . In this case the ground state degeneracy is not exact, and the symmetric state  $|0^s\rangle$  is slightly lower in energy than the antisymmetric state  $|0^a\rangle$ . We can now use this observation (that  $|0^s\rangle$  is the lowest energy state) to rewrite  $g(z)$  as

$$g(z) = \langle 0^s | \frac{d\hat{\mathcal{P}}_z}{dz} | 0^s \rangle = \lim_{t \rightarrow \infty} \frac{\langle b | \exp\{-tH\} \frac{d\hat{\mathcal{P}}_z}{dz} \exp\{-tH\} | b \rangle}{\langle b | T \exp\{-2tH\} | b \rangle}, \quad (27)$$

<sup>4</sup>The extra factor  $\frac{1}{\sqrt{2L}}$  has been included for later convenience.

<sup>5</sup>We could also consider  $\langle 0^- | \phi | 0^- \rangle$ . By reflection symmetry  $\langle 0^- | \phi | 0^- \rangle = -\langle 0^+ | \phi | 0^+ \rangle$ .

where  $|b\rangle$  is any state such that  $\langle 0^s | b \rangle$  is non-zero.

For free field theory  $g(z)$  can be exactly calculated,

$$g(z) = \sqrt{\frac{2\mu L}{\pi}} e^{-2\mu L z^2}. \quad (28)$$

For non-trivial coupling we can calculate the right-hand side of (27) using DMC methods. In Figure 2 we have plotted  $g(z)$  for  $L = 2.5\pi$  and  $L = 5\pi$ . In each case  $\frac{\lambda}{4} = 2.76$  and  $\Lambda = 4$ . All quantities are measured in units where  $\mu = 1$ . As can be seen, the distributions are bimodal and the maxima for both curves occur near  $\pm 0.55$ . We observe that the peaks are taller and narrower for larger  $L$ . This is consistent with our intuitive picture of fluctuations in the functional integral. For a small but fixed deviation in the average value of  $\phi$ , the net change in an extensive quantity such as the action or total energy scales proportionally with the size of system. Consequently the average size of the fluctuations must decrease with  $L$ . We can estimate the amplitude of the fluctuations,  $\Delta\phi$ , by assuming a quadratic dependence in  $\Delta\phi$  about the local minimum. The net effect of the fluctuation should not scale with  $L$ , and we conclude that<sup>6</sup>

$$\Delta\phi \sim \left(\frac{1}{\sqrt{L}}\right)^{\#\text{spatial dim.}} = \frac{1}{\sqrt{L}}. \quad (29)$$

This agrees with the free field result in (28) and also appears to be consistent with the peak widths plotted in Figure 2.

Let  $z_{\max}$  be the location of the non-negative maximum of  $g(z)$ . Since  $g(z)$  becomes sharply peaked as  $L \rightarrow \infty$ ,

$$\langle 0^+ | \phi | 0^+ \rangle = 2 \int_0^\infty dz z g(z) \underset{L \rightarrow \infty}{\approx} 2 z_{\max} \int_0^\infty dz g(z) = z_{\max}. \quad (30)$$

This gives us another option for calculating the vacuum expectation value. We can either integrate  $2z g(z)$  or read the location of the maximal point  $z_{\max}$ . Both will converge to the same value as  $L \rightarrow \infty$ . However, the  $z_{\max}$  result is less prone to systematic error generated by the  $O(\frac{1}{\sqrt{L}})$  fluctuations described above.<sup>7</sup> We will therefore use

$$\langle 0^+ | \phi | 0^+ \rangle = z_{\max}. \quad (31)$$

$\beta$  is defined by the behavior of the vacuum expectation value as we approach the critical coupling,

$$\langle 0^+ | \phi | 0^+ \rangle \sim (\lambda - \lambda_c)^\beta. \quad (32)$$

Using DMC methods, we have computed the  $\lambda$  dependence of the vacuum expectation value for several values of  $L$  and  $N_{\max}$ . The results are shown in the next section.

---

<sup>6</sup>The dimension of time does not enter here since we are considering properties of the vacuum, the ground state of the Hamiltonian defined at a given time. This is in contrast with lattice calculations which usually consider the quantity  $\langle \phi \rangle$ , the average of  $\phi$  over all space and time.

<sup>7</sup>We can see this explicitly in free field theory, where the vacuum expectation value should vanish.  $z_{\max} = 0$  as desired, but  $2 \int_0^\infty dz z g(z) = \frac{1}{\sqrt{2\pi\mu L}}$ .

## 4 Results

The results of our diffusion Monte Carlo simulations are presented here. For each set of parameters  $L$  and  $N_{\max}$ , the curves for  $m$  and  $\langle 0^+ | \phi | 0^+ \rangle$  near the critical coupling have been fitted using the parameterized forms

$$m = a \left( \frac{\lambda_c^m}{4!} - \frac{\lambda}{4!} \right)^\nu \quad (33)$$

and

$$\langle 0^+ | \phi | 0^+ \rangle = b \left( \frac{\lambda}{4!} - \frac{\lambda_c^{(\phi)}}{4!} \right)^\beta. \quad (34)$$

For the mass curves, data points with  $m \lesssim L^{-1}$  have correlation lengths exceeding the size of our system and are of questionable significance. We have therefore fit these curves two different ways, once using all data points and a second time excluding small  $m$  values. The curves for the data set  $L = 2.5\pi$  and  $N_{\max} = 10$  are shown in Figures 3 and 4.<sup>8</sup> The error bars represent an estimate of the error due to Monte Carlo statistical fluctuations and, in the case of the mass data, pollution due to higher energy states. Let  $\tilde{\chi}_d^2$  denote the reduced chi-squared value for  $d$  degrees of freedom. The results of the fits are as follows:

$L = 2.5\pi$ ,  $N_{\max} = 8$  ( $\Lambda = 3.2$ ):

$$\begin{aligned} \frac{\lambda_c^m}{4!} &= 3.1 \pm 0.2, \quad \nu = 1.1 \pm 0.1, \quad a = 0.31 \pm 0.02, \quad \tilde{\chi}_{15}^2 = 0.81 \text{ (all)}, \\ \frac{\lambda_c^m}{4!} &= 3.1 \pm 0.2, \quad \nu = 1.0 \pm 0.1, \quad a = 0.30 \pm 0.03, \quad \tilde{\chi}_8^2 = 0.96 \text{ (partial)}, \\ \frac{\lambda_c^{(\phi)}}{4!} &= 2.5 \pm 0.1, \quad \beta = 0.15 \pm 0.02, \quad b = 0.65 \pm 0.05, \quad \tilde{\chi}_8^2 = 0.45 \end{aligned} \quad (35)$$

$L = 2.5\pi$ ,  $N_{\max} = 10$ , ( $\Lambda = 4$ ):

$$\begin{aligned} \frac{\lambda_c^m}{4!} &= 2.9 \pm 0.2, \quad \nu = 1.1 \pm 0.1, \quad a = 0.35 \pm 0.02, \quad \tilde{\chi}_{12}^2 = 0.46 \text{ (all)}, \\ \frac{\lambda_c^m}{4!} &= 2.9 \pm 0.2, \quad \nu = 1.0 \pm 0.1, \quad a = 0.37 \pm 0.03, \quad \tilde{\chi}_6^2 = 0.37 \text{ (partial)}, \\ \frac{\lambda_c^{(\phi)}}{4!} &= 2.5 \pm 0.1, \quad \beta = 0.18 \pm 0.01, \quad b = 0.70 \pm 0.03, \quad \tilde{\chi}_9^2 = 0.29 \end{aligned} \quad (36)$$

$L = 5\pi$ ,  $N_{\max} = 16$ , ( $\Lambda = 3.2$ ):

$$\begin{aligned} \frac{\lambda_c^m}{4!} &= 3.0 \pm 0.2, \quad \nu = 1.2 \pm 0.1, \quad a = 0.32 \pm 0.03, \quad \tilde{\chi}_{13}^2 = 0.87 \text{ (all)}, \\ \frac{\lambda_c^m}{4!} &= 3.1 \pm 0.2, \quad \nu = 1.2 \pm 0.1, \quad a = 0.30 \pm 0.03, \quad \tilde{\chi}_{10}^2 = 0.88 \text{ (partial)}, \\ \frac{\lambda_c^{(\phi)}}{4!} &= 2.7 \pm 0.1, \quad \beta = 0.12 \pm 0.02, \quad b = 0.62 \pm 0.04, \quad \tilde{\chi}_6^2 = 0.50 \end{aligned} \quad (37)$$

$L = 5\pi$ ,  $N_{\max} = 20$ , ( $\Lambda = 4$ ):

$$\begin{aligned} \frac{\lambda_c^m}{4!} &= 2.8 \pm 0.2, \quad \nu = 1.2 \pm 0.1, \quad a = 0.35 \pm 0.06, \quad \tilde{\chi}_{11}^2 = 1.2 \text{ (all)}, \\ \frac{\lambda_c^m}{4!} &= 2.9 \pm 0.2, \quad \nu = 1.3 \pm 0.1, \quad a = 0.36 \pm 0.06, \quad \tilde{\chi}_8^2 = 1.1 \text{ (partial)}, \\ \frac{\lambda_c^{(\phi)}}{4!} &= 2.5 \pm 0.1, \quad \beta = 0.11 \pm 0.02, \quad b = 0.65 \pm 0.04, \quad \tilde{\chi}_8^2 = 0.88. \end{aligned} \quad (38)$$

---

<sup>8</sup>As mentioned before, we are using units where  $\mu = 1$ .



These results are subject to errors due to the finite size  $L$  and finite cutoff scale  $\Lambda$ . We will use our data for different values of  $L$  and  $\Lambda$  to extrapolate to the limit  $L \rightarrow \infty, \Lambda \rightarrow \infty$ . For the parameters  $\nu, a, \beta, b$  we use the naive asymptotic form

$$x(L, \Lambda) = x + \frac{1}{\Lambda^2} x_{\Lambda^2} + \frac{1}{L^2} x_{L^2} + \dots \quad (39)$$

For the critical couplings  $\lambda_c^m$  and  $\lambda_c^{(\phi)}$ , however, we modify the finite  $L$  correction according to the finite-size scaling hypothesis [6]

$$\lambda(L, \Lambda) = \lambda + \frac{1}{\Lambda^2} \lambda_{\Lambda^2} + \frac{1}{|L|^{1/\nu}} \lambda_{|L|^{1/\nu}} + \dots \quad (40)$$

The results we find are<sup>9</sup>

$$\begin{aligned} \frac{\lambda_c^m}{4!} &= 2.5 \pm 0.2 \pm 0.1, \quad \nu = 1.3 \pm 0.2 \pm 0.1, \quad a = 0.43 \pm 0.05 \pm 0.02 \text{ (all)}, \quad (41) \\ \frac{\lambda_c^m}{4!} &= 2.3 \pm 0.2 \pm 0.1, \quad \nu = 1.4 \pm 0.2 \pm 0.1, \quad a = 0.48 \pm 0.06 \pm 0.02 \text{ (partial)}, \\ \frac{\lambda_c^{(\phi)}}{4!} &= 2.5 \pm 0.1 \pm 0.1, \quad \beta = 0.13 \pm 0.02 \pm 0.01, \quad b = 0.71 \pm 0.04 \pm 0.03. \end{aligned}$$

The first error bounds include inaccuracies due to Monte Carlo statistics, higher energy states (for the mass curves), and extrapolation. The second error bounds represent estimates of the systematic errors due to our choice of initial state, time step parameter, and bin sizes in the DMC simulations. For data generated from the mass curves, the main source of error was due to extrapolation. The extrapolation error for the vacuum expectation value data was still the most significant, though considerably smaller than that for the mass calculations. This reduction is probably a result of the method used to measure the vacuum expectation value.<sup>10</sup> Our results for the critical exponents are consistent with the Ising model predictions

$$\nu = 1, \quad \beta = \frac{1}{8}. \quad (42)$$

The results for the critical coupling  $\frac{\lambda_c^m}{4!}$  and  $\frac{\lambda_c^{(\phi)}}{4!}$  are in agreement with the recently obtained lattice result [7]<sup>11</sup>

$$\frac{\lambda_c}{4!} = 2.56_{-.01}^{+.02}. \quad (43)$$

## 5 Summary

We have discussed the generalization of spherical field theory to other modal expansion methods, in particular, periodic field theory. Using periodic field

<sup>9</sup>Due to the relatively weak dependence on  $L$  and  $\Lambda$ , the reduced chi-squared values for our extrapolation fits are quite small ( $\ll 1$ ) and do not provide a useful statistical measure.

<sup>10</sup>We are referring to the result  $\langle 0^+ | \phi | 0^+ \rangle = z_{\max}$ , which eliminates peak broadening effects for finite  $L$ . This is discussed at the end of the previous section.

<sup>11</sup>Critical exponents were not measured in this study.

methods we have analyzed two-dimensional  $\phi^4$  theory and computed the critical coupling and critical exponents  $\nu$  and  $\beta$  associated with spontaneous breaking of  $\phi \rightarrow -\phi$  reflection symmetry. Our value of the critical coupling is in agreement with a recent lattice calculation, and our values for the critical exponents are consistent with the critical exponents of the two-dimensional Ising model. This lends support to the popular belief that the two theories belong to the same universality class.

The full set of diffusion Monte Carlo computations used in our analysis required about 30 hours on a 350 MHz PC processor. Complete codes can be obtained upon request from the authors. The required computational time appears to be dominated by the number of operations required to update the Hamiltonian, which scales as  $N_{\max}^2$ . Errors can be reduced quite substantially by using larger values of  $L$  and  $N_{\max}$  and utilizing large-scale parallel processing. No less important, however, is that periodic field theory provides a simple and efficient approach to studying non-perturbative phenomena with only modest computer resources. Improvements are now under way to utilize fast Fourier transform methods [8] and increase the computational speed. Future studies have been planned to analyze phase transitions in other field theory models.

## Acknowledgment

We are grateful to Eugene Golowich for useful advice and discussions. We also thank Jon Machta for comments on finite-size scaling and the referee of the original draft for suggesting several improvements. Support provided by the National Science Foundation under Grant 5-22698.

## References

- [1] D. Lee, Phys. Lett. B439 (1998) 85.; D. Lee, Phys. Lett. B444 (1998) 474.; B. Borasoy, D. Lee, Phys. Lett. B447 (1999) 98; D. Lee, N. Salwen, hep-th/9905077.
- [2] M. Chaichian, A. Demichev, P. Prešnajder, hep-th/9904132.
- [3] J. Glimm, A. Jaffe, Phys. Rev. D10 (1974) 536; J. Glimm, A. Jaffe, T. Spencer, Comm. Math. Phys. 45 (1975) 203.
- [4] S. Chang, Phys. Rev. D13 (1976) 2778.
- [5] I. Kosztin, B. Faber, K. Schulten, Amer. J. Phys. 64 (1996) 633.
- [6] M. Fisher, M. Barber, Phys. Rev. Lett. 28, 1516 (1972).
- [7] W. Loinaz, R. Willey, Phys. Rev. D58 (1998) 076003.
- [8] J. Kogut, J.-F. Lagaë, Nucl. Phys. Proc. Suppl. 34 (1994) 552.

## Figures

Figure 1. The only divergent diagram, which can be cancelled by normal ordering.

Figure 2. Plot of  $g(z)$  for  $L = 2.5\pi$  and  $L = 5\pi$ . In each case  $\frac{\lambda}{4\Gamma} = 2.76$  and  $\Lambda = 4$ .

Figure 3. Plot of  $m$  as a function of  $\frac{\lambda}{4\Gamma}$  for  $L = 2.5\pi$ ,  $N_{\max} = 10$ .

Figure 4. Plot of  $\langle 0^+ | \phi | 0^+ \rangle$  as a function of  $\frac{\lambda}{4\Gamma}$  for  $L = 2.5\pi$ ,  $N_{\max} = 10$ .

Figure 1

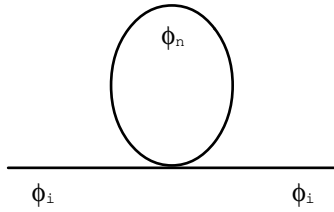


Figure 2

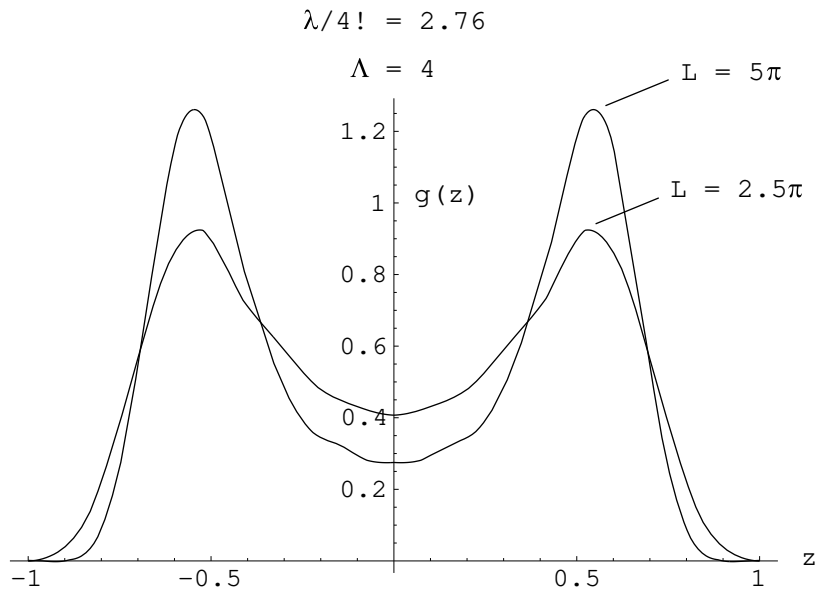


Figure 3

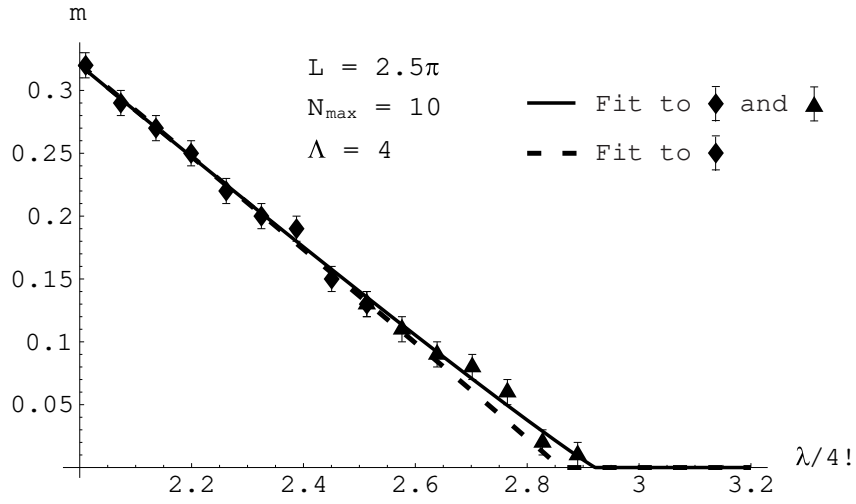


Figure 4

